Experimental Investigation of Wave Breaking Criteria Based on Wave Phase Speeds

PAUL STANSELL

Department of Civil and Offshore Engineering, Heriot-Watt University, Edinburgh, Scotland

COLIN MACFARLANE

Department of Ship and Marine Technology, University of Strathclyde, Glasgow, Scotland

(Manuscript received 26 May 2000, in final form 16 August 2001)

ABSTRACT

Experiments were performed that test the kinematic breaking criterion, which states that the horizontal fluid particle velocity at the surface of a crest *exceeds* the local phase speed of the crest *prior* to breaking. Three different definitions of phase speed are used to calculate phase velocities of the wave crests from detailed surface elevation measurements. The first definition, based on the equivalent linear wave, is constant over the wavelength of the wave. The second, based on partial Hilbert transforms of the surface elevation data, is local in space and time giving instantaneous values at all space and time measurements. The third, based on the speed of the position of the crest maximum, is local in time but not in space. Particle image velocimetry is used to obtain horizontal components of fluid particle velocity at the surface of crests of breaking and nonbreaking waves produced in a wave flume using the chirp-pulse focusing technique. The ratios of these fluid particle speeds to crest phase speeds are calculated and are consistently less than unity. The speed ratio for the rounded crest of a plunging breaker is at most 0.81, implying that the kinematic breaking criterion is far from satisfied. The ratio for the more sharply pointed crest of a spilling breaker is at most 0.95, implying that the kinematic breaking criterion is closer to being satisfied. Thus, for the breaking waves in this study the kinematic breaking criterion is not satisfied for any of the three definitions of phase speed and so it cannot be regarded as a universal predictor of wave breaking.

1. Introduction

The breaking of surface gravity waves is an important phenomenon. It is one of the most significant energy redistribution terms in ocean wave models. It contributes to wave damping, horizontal momentum transport from waves to currents, and sediment transport in coastal waters. The prediction of hydrodynamic loads on structures in the ocean are dependent on the velocity and acceleration of the fluid particles, and in breaking waves these are far greater than those found in nonbreaking waves of the same height (Melville and Rapp 1988). Yet, despite their importance, breaking waves in irregular seas are still poorly understood. Many authors have proposed breaking criteria (by which we mean a parameter that can, in principle at least, be measured in the region of a wave crest and for which a threshold crossing would imply that the wave is breaking or about to break). One criterion that is often suggested is that any surface gravity wave will break if the ratio of the horizontal fluid particle velocity in the crest to the phase speed of the crest is greater than unity.

This hypothesis has been stated as early as Rankine (1864), by Kinsman (1984, section 5.4), Kjeldsen (1990), Tulin and Li (1992), and as recently as Banner and Peregrine (1993, p. 386) where they say that:

> The traditional [kinematic] criterion for wave breaking is that horizontal water velocities must exceed the speed of the crest. This appears self evident, but from detailed flow fields it is found that since the crest shape is changing there is often no precisely relevant crest velocity. Rather, there is a range of velocities which roughly correspond to the crest speed, and water velocities usually exceed these by appreciable margins.

Nevertheless, it seems that this kinematic criterion for wave breaking has not been verified, either experimentally or computationally. Indeed, Melville and Rapp (1988) state in their introduction that what motivated their paper was the ''desire to identify breaking by searching for events in which the fluid velocity at the surface exceeded the phase velocity of the wave'' but in the body of the paper they ''did not pursue this comparison of phase and fluid velocities.''

There exists some confusion and contradiction con-

Corresponding author address: Dr. Paul Stansell, Department of Civil and Offshore Engineering, Heriot-Watt University, Riccarton, Edinburgh EH14 4AS, Scotland.
E-mail: p.stansell@hw.ac.uk

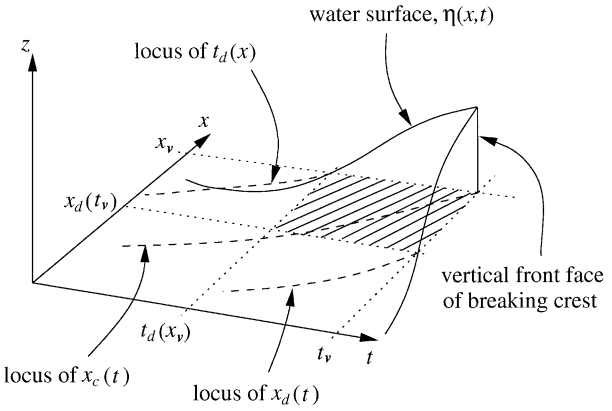

FIG. 1. Schematic diagram of the parameters used in the defining equation, Eq. (1), of the kinematic breaking criterion. The hatched region on the (x, t)-coordinate plane, $x_d(t_v) < x < x_v$, $t_d(x_v) < t < t_v$, is the region in which the criterion is expected to hold at least one point.

cerning this issue in the literature, where the universality of the kinematic breaking criterion is often assumed correct without question. In this study, we set out to investigate this claim directly. We pose the following question: is it a necessary condition of wave breaking that, at or shortly before the time of breaking and within the spatial extent of the crest, there exist horizontal fluid particle velocities that *exceed* the phase speed of the crest? To express this question mathematically we define the z direction to be that of the outward normal to the undisturbed fluid surface and the x direction to be in the plane of the undisturbed fluid surface. The position and time of the inception of a breaking wave is defined to be the position and time of the first occurrence of a vertical tangent to the front face to the wave and is denoted by (x_v, t_v). The above statement of the kinematic breaking criterion can now, for a wave traveling in the positive x direction, be written as

$$u[z = \eta(x, t), x, t] > c_p(x, t)$$

$$\text{for } x_d(t_v) < x < x_v,\ t_d(x_v) < t < t_v, \qquad (1)$$

where $u(z, x, t)$ is the x component of fluid particle velocity in the coordinate plane (z, x), $\eta(x, t)$ is the z coordinate of the fluid's free surface at (x, t), t is the time, $x_d(t)$ is the position of the first zero up-crossing behind the wave crest parameterized by time, $t_d(x_v)$ is the time of the first zero up-crossing behind the wave crest parameterized by position, and $c_p(x, t)$ is some appropriate definition of the wave's phase speed. A schematic diagram illustrating this definition is shown in Fig. 1.

As suggested by Banner and Peregrine (1993), applying the kinematic breaking criterion to an irregular wave is complicated by the difficulty in defining or measuring the phase speed of a wave that is not of permanent form. To overcome this problem we require a way of defining properties of the wave that are local in space and time. We achieve this in section 2 by proposing a particular definition of phase speed based on the partial Hilbert transforms of the surface elevation of a wave, $\eta(x, t)$. The definition can be applied to obtain a number that can be said to represent the local phase speed of the wave. It can be applied to nonlinear wave forms that are evolving rapidly in space and time. It is truly local in the sense that the phase speed so calculated is a function of both space and time and so can yield different values of phase speed for different positions and times within the same wave. A discussion of related work is deferred until section 3. In section 4 we compare local phase speed values, nonlocal phase speed values obtained from the equivalent linear wave, and phase speed values from another definition local only in time, with the horizontal fluid particle velocities measured at the surface of breaking and nonbreaking wave crests. Finally, in sections 5 and 6 we offer overall discussions and conclusions.

2. Three definitions of phase speed

From the profile a train of irregular gravity waves evolving in space and time on the surface of a fluid it is not straightforward to define the speed of any particular wave at any particular arbitrary point in space and time. Thus, we begin by proposing three possible definitions.

Our first definition of phase speed is that based on a simple approach commonly used in ocean studies. We define the nonlocal phase speed of an irregular surface wave as the speed of an equivalent linear wave. For a linear wave consisting of a single Fourier component we can always find a frame of reference in which the wave is stationary. From this observation we can define the phase speed of the wave, c_p, to be minus the speed of the moving reference frame. Thus, for the linear wave $\eta(x, t) = a\cos(kx - \omega t)$, where $k = 2\pi/\lambda$ is the wavenumber, $\omega = 2\pi f$ is the angular frequency, λ is the wavelength, $f = 1/T$ is the frequency, and T is the period, we define

$$c_p = \frac{\omega}{k}. \qquad (2)$$

Application of this definition to an irregular wave (for which a stationary frame of reference does not exist) requires the approximation that the values of T and λ are constant over the time and space scale of any particular wave of interest. To calculate the phase speed of the equivalent regular wave the required values of T and λ can be measured as the time and distance between consecutive zero-downcrossings on the irregular wave profile's time series and space series. If, as is common, only the time series of the surface profile is known, then a dispersion relation, such as that for deep water,

$$\omega^2 = gk, \qquad (3)$$

where g is the acceleration due to gravity, can be invoked to eliminate k from Eq. (2).

Application of this simple definition of the phase speed to a wave that is about to break is not satisfactory since, for example, the speed of the breaking crest must be greater than the speed of the trough preceding it if the front face of the wave is to become vertical. By this simple definition of c_p, however, the phase speed is identical at all points between consecutive zero-downcrossings of a wave. Thus, for a breaking wave it is not acceptable to consider ω and k constant over the time and length scales of the wave as defined by the positions of the zero-downcrossings.

To overcome this problem we propose a second, instantaneous or local, definition of phase speed as the ratio of an instantaneous angular frequency, $\omega(x, t)$, with an instantaneous wavenumber, $k(x, t)$. That is

$$c_p(x, t) \equiv \frac{\omega(x, t)}{k(x, t)}. \tag{4}$$

The theory of analytic functions provides a convenient way to define $\omega(x, t)$ and $k(x, t)$. For a two-dimensional wave (one time and one space dimension) denoted $\eta(x, t)$, we require the defining equations for the partial Hilbert transforms of this arbitrary two-dimensional function with respect to x and t. These are, respectively [see, e.g., chapter 7 of Poularikas (1995)],

$$H_x[\eta(x, t)] = \frac{1}{\pi} P \int_{-\infty}^{\infty} \frac{\eta(x', t)}{(x - x')}\, dx', \tag{5}$$

$$H_t[\eta(x, t)] = \frac{1}{\pi} P \int_{-\infty}^{\infty} \frac{\eta(x, t')}{(t - t')}\, dt', \tag{6}$$

where P stands for the Cauchy principal value of the integral. Using Eq. (5), we define the local wavenumber by

$$k(x, t) \equiv \frac{\partial}{\partial x}\phi_x(x, t), \tag{7}$$

where the phase function $\phi_x(x, t)$ is given by

$$\tan\phi_x(x, t) = \frac{H_x[\eta(x, t)]}{\eta(x, t)}. \tag{8}$$

Differentiating with respect to x gives

$$\frac{\partial\phi_x}{\partial x} = \frac{\cos^2\phi_x}{\eta^2}\left(\eta\frac{\partial}{\partial x}H_x[\eta] - H_x[\eta]\frac{\partial}{\partial x}\eta\right). \tag{9}$$

From Eq. (8) we see that $\cos^2\phi_x = \eta^2/(\eta^2 + H_x^2[\eta])$, which along with Eqs. (7) and (9), gives the following expression for the local wavenumber

$$k(x, t) = \frac{1}{\eta^2 + H_x^2[\eta]}\left(\eta\frac{\partial}{\partial x}H_x[\eta] - H_x[\eta]\frac{\partial}{\partial x}\eta\right). \tag{10}$$

In an analogous fashion, but starting from Eq. (6) and defining the local angular frequency by

$$\omega(x, t) \equiv \frac{\partial}{\partial t}\phi_t(x, t), \tag{11}$$

where the phase function $\phi_t(x, t)$ is given by

$$\tan\phi_t(x, t) = \frac{H_t[\eta(x, t)]}{\eta(x, t)}, \tag{12}$$

we can write $\omega(x, t)$ as

$$\omega(x, t) = \frac{1}{\eta^2 + H_t^2[\eta]}\left(\eta\frac{\partial}{\partial t}H_t[\eta] - H_t[\eta]\frac{\partial}{\partial t}\eta\right). \tag{13}$$

From Eqs. (4), (10), and (13) a general expression for a phase speed local in space and time is

$$c_p(x, t) = \frac{\eta^2 + H_x^2[\eta]}{\eta^2 + H_t^2[\eta]}\left(\frac{\eta\dfrac{\partial}{\partial t}H_t[\eta] - H_t[\eta]\dfrac{\partial}{\partial t}\eta}{\eta\dfrac{\partial}{\partial x}H_x[\eta] - H_x[\eta]\dfrac{\partial}{\partial x}\eta}\right). \tag{14}$$

Note that in the linear (small amplitude or Airy wave) approximation $H_t[\eta] = -H_x[\eta]$, which simplifies the expression for the local phase speed to

$$c_p(x, t) = \frac{\eta\dfrac{\partial}{\partial t}H_t[\eta] - H_t[\eta]\dfrac{\partial}{\partial t}\eta}{H_t[\eta]\dfrac{\partial}{\partial x}\eta - \eta\dfrac{\partial}{\partial x}H_t[\eta]}.$$

Use of the Hilbert transform to define the instantaneous frequency and wavenumber in this way is not new and is considered by some as controversial, particularly for functions with wideband spectra. For such functions values of the frequency may be obtained that are zero or even negative. Such results are regarded by some as unphysical. They are associated with maxima in $\eta(x, t)$ occurring below, or minima occurring above, the mean water level. These large fluctuations have been observed and explained in some detail by Melville (1983, section 4.3). In this study we are only interested in obtaining the instantaneous frequencies (and wavenumbers) in a relatively small time (or space) domain in close vicinity to the crest of the wave where problematic zero and negative values of the local frequencies and wavenumbers are not present.

The third working definition of phase speed that we use is defined as the speed of the position of the surface elevation maximum associated with the wave crest of interest (see, e.g., Baldock et al. 1996). Letting $x_c(t)$ denote the x coordinate of the surface maximum of the crest then its phase speed, local only in the time dimension, is defined to be

$$c_p(t) \equiv \frac{dx_c(t)}{dt}. \tag{15}$$

This definition of phase speed is only valid at the locus of the crest maximum given by $[x_c(t), t]$ and is therefore instantaneous only in time, not in space.

Note the use of the arguments to distinguish the three definitions of phase speed given by Eqs. (2), (14), and (15).

3. Survey of related work

In this section we review previous studies and show how none of them answer the question associated with Eq. (1). We discuss three studies that used the Hilbert transform of the surface elevation to definite local angular frequency and wavenumber for irregular waves. We also review some studies, both experimental and computational, that compare measured fluid particle velocities in a breaking crest with some definition of phase speed. Inconsistency in the results is evident. It will be seen that each of these studies invoked linear theory at some point. As far as we are aware, of each of the studies that test the kinematic breaking criterion, ours is the only one in which measurements of $c_p(x, t)$ and u are made that avoid any linear approximations. This represents an important aspect of this study which differentiates our results from those of other studies, especially given the highly nonlinear nature of breaking waves.

We end this section with a discussion of some relevant points from the theory of regular (Stokes) waves.

a. Irregular waves

The problem of defining a fully local wave speed for an irregular wave was tackled by Melville (1983). In his experiments Melville (1983) started with the generation of a 2-Hz sinusoidal wave train at the wave generator. At a fixed point, x_1, the surface elevation of these waves, $\eta(x_1, t)$, was sampled at a rate up to 200 Hz. The wave train evolved toward an irregular breaking wave and the Hilbert transform (with respect to time) of $\eta(x_1, t)$ was used to calculate the phase function $\phi_t(x_1, t)$ by Eq. (12). The instantaneous angular frequency at position x_1, $\omega(x_1, t)$, was then calculated from Eq. (11). To obtain a local wavenumber Melville (1983) took the Hilbert transforms (with respect to time) of two closely spaced measurements, $\eta(x_1 - \Delta x/2, t)$ and $\eta(x_1 + \Delta x/2, t)$, to obtain the phase functions $\phi_t(x_1 - \Delta x/2, t)$ and $\phi_t(x_1 + \Delta x/2, t)$ from Eq. (12). These were then used to define an instantaneous wavenumber at x_1

$$k(x_1, t) = \frac{\phi_t(x_1 + \Delta x/2, t) - \phi_t(x_1 - \Delta x/2, t)}{\Delta x} \approx \left[\frac{\partial}{\partial x}\phi_t(x, t)\right]_{x=x_1}. \quad (16)$$

This is not the same as the definition of $k(x, t)$ given in Eq. (7), so the local phase speed defined by Melville (1983) as the quotient $\omega(x_1, t)/k(x_1, t)$ is not the same as that given by Eq. (4). It is the present authors' opinion that a general definition of local wavenumber based on the gradient of the phase function $\phi_t(x_1, t)$, as given by Eq. (16), is flawed in that it is an approximation when applied to the case of a finite amplitude wave. It is valid in the linear wave limit, that is to say, the limit of infinitesimal wave amplitude. This is because for a wave composed of a linear superposition of Airy waves $H_t[\eta(x, t)] = -H_x[\eta(x, t)]$. [Further discussion on this point is given in relation to Hwang et al. (1989, p. 22).] Melville (1983), however, does not compare his local phase speed with fluid particle velocities.

A numerical study that used the Hilbert transform of the surface elevation to define local aspects of irregular breaking and nonbreaking waves was performed by Banner and Tian (1998). Boundary integral simulations of fully nonlinear surface waves were used to assess the behavior of nondimensional relative rates of change of local mean energy and momentum densities following their envelopes. The definition of these local variables required the calculation of the instantaneous wavelength and frequency of the wave, although, in their final calculation, the authors used the frequency of a linear wave as an approximation to the local frequency defined by Eq. (14). Their results show that, if the nondimensional growth rates exceed 0.2, then the growth rate and the envelope become phase locked for a sufficient time for the associated surface wave to acquire enough energy and momentum to break. For nondimensional growth rates that do not exceed 0.2 the growth rate oscillates on a faster timescale than the envelope and thus no phase locking occurs and there is continual growth and decay in energy and momentum of the associated surface wave, which therefore does not break. The study suggests that a growth rate value exceeding the threshold of 0.2 would predict the onset of breaking universally.

As with Melville (1983), when calculating the local wavelength and local angular frequency Banner and Tian (1998) do not distinguish between the partial Hilbert transform with respect to x or t of the surface profile $\eta(x, t)$. If they use the partial Hilbert transform with respect to x then their calculation of $k(x, t)$ will be correct but that of $\omega(x, t)$ may be incorrect. Their calculations of $\omega(x, t)$ may include errors from two sources: that due to the difficulty in calculating the Hilbert transforms after time t_v when $\eta(x, t)$ becomes triple valued and that due to the restriction imposed on the time domain integration, required for the calculation of the partial Hilbert transform with respect to time, by the boundary integral method, which breaks down a short time later when the tip of the overturning crest touches the forward face of the wave. It is interesting to note that in the final implementation of their definition, instead of the instantaneous angular frequency $\omega(x, t)$, they use the constant value given by ω for the equivalent linear wave.

1) KINEMATIC BREAKING CRITERION VIA NUMERICAL SIMULATIONS

Boundary integral simulations of breaking waves from which one can compare the fluid velocities with

equivalent linear wave phase speeds have been performed by Vinje and Brevig (1981) and New et al. (1985). Vinje and Brevig made comparisons, for deep and shallow water cases, of $u[\eta(x, t), x, t]$ within crests of plunging breakers and phase velocities, c_p, calculated from an equivalent linear wave. From the two plots in their Fig. 4, which show shallow and deep water plunging breakers at time t_v, one can see that $u[z = \eta(x, t_v), x, t_v] < c_p$ for all x. Only from plots in their Fig. 6, which show the deep water plunging breaker at times $t > t_v$ do we see $u[z = \eta(x, t), x, t] > c_p$ for some x and t.

New et al. (1985) performed simulations of plunging breakers in water of finite depth and achieved results for shallow water that compare favorably with those of Vinje and Brevig (1981). New et al.'s (1985) Figs. 7b and 8b, that illustrate their Wave 3, show that $u[\eta(x, t), x, t]$ in the crest of the breaking wave at about the time of the first occurrence of a vertical tangent to the surface profile is almost equal to the phase speed, c_p, of the equivalent linear wave.[1] Subsequently, as the ejected jet grows, $u[\eta(x, t), x, t]$ in the crest certainly increases to a value greater than c_p.

Thus, it seems that neither the simulations of Vinje and Brevig (1981) nor those of New et al. (1985) confirm the kinematic breaking criterion, as defined by Eq. (1), when using an equivalent linear wave to define the phase speed.

2) Kinematic breaking criterion via wave flume experiments

Melville and Rapp (1988), Kjeldsen (1989), Perlin et al. (1996), and Chang and Liu (1998) have all performed wave flume experiments to measure the fluid particle velocities in the crests of breaking waves.

Melville and Rapp used laser anemometry to measure the fluid particle velocities on the surface of breaking waves by seeding the surface with neutrally buoyant tracer particles. In their Fig. 3, which shows the surface profile and $u[\eta(x, t), x, t]$, we see that the maximum value of u/c measured in the breaking wave is about 0.575, where $c = g/\omega$ is their definition of linear wave speed.

Kjeldsen (1989) used two different methods to measure the fluid velocities in the crests of plunging breakers after they had overturned but before their tips touched the forward face. For the first method, a current meter was moved along with the wave crest; for the second, high-speed films of the plunging breaker were taken from which the fluid velocity normal to the surface of the overturning crest was calculated. In both cases Kjeldsen measured $u(z, x, t)$ in the crest that exceeded the equivalent linear wave phase speed, c_p, but in both cases the waves had already overturned, $t > t_v$, making redundant the concept of using the ratio u/c_p as a breaking criterion. Examining Kjeldsen's (1989) Fig. 13, one sees that the fluid particle velocity near the vertical part of the front face of the breaking wave is very low, at about 0.3 of the linear phase speed, whereas near the highest point of the crest it is very much higher, at about 1.36 of the linear phase speed. Doubt is cast on Kjeldsen's experimental results when comparing them with the numerical simulations of Vinje and Brevig (1981) and Longuet-Higgins and Cokelet (1976) or the experimental and numerical results of Skyner (1996), each of whom show a more gradual change in fluid particle velocity as one moves up the vertical front face to the high point or tip of the plunging breaker.

Perlin et al. (1996) used particle image velocimetry (PIV) and particle tracking velocimetry (PTV) to measure the fluid particle velocities in the crests of plunging breakers. These velocities were compared to wave crest phase speeds calculated from the equivalent linear wave, and also the crest high-point definition [Eq. (15)]. The greatest value of $u(z, x, t)$ was measured by PTV in the ejecting jet of the overturning wave. The value was 130% of the equivalent linear wave phase speed, c_p. However, the greatest value of $u(z, x, t)$ measured *before* the wave overturned was measured by PIV in a crest "with the front face nearly vertical." The value was 74% of the phase speed.

Chang and Liu (1998) used a phase velocity calculated from linear theory and $u(z, x, t)$ measurements obtained from PIV. They find that, when the wave is "close to breaking" (before the front face is vertical), the maximum velocity is 0.86 times the linear phase speed, c_p. After the wave has overturned they measure the maximum velocity in the ejecting jet as 1.07 times c_p.

Thus, in none of the experimental studies performed by Melville and Rapp (1988), Kjeldsen (1989), Perlin et al. (1996), or Chang and Liu (1998) are values $u(z, x, t)$ measured that *exceed* the phase speed of the equivalent linear wave before the inception of breaking (that is to say, for $t < t_v$). Thus, because none of these studies measure $u > c_p$ for $t < t_v$, the kinematic breaking criterion, as defined by Eq. (1), is not supported by any of these studies.

Hwang et al. (1989) performed wave flume experiments that measured only the surface wave profile, $\eta(t)$, at a single point in space. The fluid particle velocities were not measured directly. Instead they obtained values for the x component of the fluid particle velocity at the fluid surface from, in our notation,

$$u = \frac{\partial}{\partial t} H_t[\eta(t)], \tag{17}$$

which only gives a correct value for u in the linear wave theory approximation. They do, however, define a local phase velocity similar, but not identical, to that defined

[1] The phase speed of the equivalent linear wave is calculated by Eqs. (2) and (3) as $c_p \approx 0.4$ since $\lambda = g = 1$ in New et al.'s (1985) simulations.

by Eq. (14). The difference is their need to define local wavelength by

$$k(x, t) = \frac{\partial}{\partial x}\phi_t(x, t)$$

instead of by Eq. (7). Their definition is only valid when $\phi_t(x, t) = \phi_x(x, t)$, which again only occurs in the linear approximation. Although Hwang et al. (1989) do measure $u > c_p$, it is not clear whether their measurements were made in the ejecting jet, that is to say, at times greater than t_v. Also, they used linear theory to predict the fluid velocities by Eq. (17), and it is well known that linear theory overestimates the magnitude of the horizontal fluid velocities above the mean water level (Gudmestad et al. 1988; Skjelbreia et al. 1991; Gudmestad 1993).

b. Regular waves

The discussion so far has been concerned exclusively with irregular waves. For regular irrotational waves (Stokes waves) the situation is different. Instabilities that lead regular waves to break have been studied in some detail during the last three decades. Longuet-Higgins (1978a,b) has shown by a linear perturbation analysis that Stokes waves are unstable to certain superharmonic and subharmonic normal-mode amplitude perturbations. Longuet-Higgins and Cokelet (1978) investigated the growth of these instabilities numerically and showed that they do indeed lead to breaking. By considering just a single isolated crest of a steep (''almost highest'') Stokes wave Longuet-Higgins and Cleaver (1994) have shown, again by a linear perturbation analysis, that the crest is unstable, having a normal mode perturbation with an exponential growth rate. Longuet-Higgins and Dommermuth (1997) found a second normal mode of crest instability and traced the development of the fastest growing instability of the almost-highest wave numerically, showing that these instabilities cause the crest to overturn.

The existence of crest instabilities is important because it establishes that there is an instability that is essentially a local property of the wave crest and hence may occur in other types of waves such as irregular waves. These crest instabilities, however, are not likely to account for all types of wave breaking. Longuet-Higgins and Tanaka (1997) say in conclusion that their results can only apply to wind waves in a limiting sense as a typical ocean wave spectrum displays strong wave grouping and a wide range of length scales and both of these features will be associated with other types of wave instability.

The purpose of the present study is to examine the kinematic wave breaking criterion that is said to apply to wave crests universally. Indeed, it was from the conjectured equivalence of horizontal particle velocity and phase speed applied to a limiting regular wave that Stokes derived other aspects of the limiting regular wave such as its 120° crest angle [see, e.g., p. 189 of Cokelet (1977)]. Equivalence of phase speed and fluid particle speed in the crest is a logical conjecture for a periodic wave that has a sharply pointed crest. A limiting periodic wave has a sharp corner flow (with zero radius of curvature) at the tip of the crest and surface of the fluid is a streamline. Viewing the wave from a reference frame in which the surface profile is stationary (that is to say, a frame moving at the phase speed of the wave) the flow at the tip of the crest must be a stagnation point in order to avoid infinite fluid particle accelerations. Hence, the velocity of the fluid particle at the tip of the sharp crest must be equal to the speed of the wave profile.

The work of Longuet-Higgins and others (cited above) does not contradict or falsify the kinematic breaking criterion. At first sight it may appear to do so since it shows that a Stokes wave becomes unstable before it reaches its limiting form where the equivalence of phase speed and fluid particle speed in the crest is certain. But the perturbations applied to the almost-highest wave by Longuet-Higgins and Cleaver (1994) are not stationary in the frame of reference traveling with the phase speed of the underlying Stokes wave. Thus, the perturbations will not only affect the velocity field of the surface of the wave, but, more importantly to our discussion, the previously global phase speed of the underlying Stokes wave will be replaced by the local phase speed of the perturbed Stokes wave. The relationship between the local phase speed and the fluid particle velocities on the surface of the unstable Stokes wave is not clear.

4. Wave flume experiments with nonlinear waves

a. Experimental apparatus and measurements

Wave experiments were carried out in a wave flume facility belonging to the Fluids Group at the University of Edinburgh, Scotland. The flume had a horizontal bottom and was 9.77 m long by 0.4 m wide with a still water depth of 0.75 m. The x coordinate was measured along the flume from the front of the vertical wave paddle, and the z coordinate upward from the still water level. Waves were produced at one end of the flume by a computer-controlled hinged wave paddle. The paddle control incorporated a force feedback signal that enabled it to partially absorb any waves reflected from the opposite end of the flume. At the opposite end of the flume was a passive wave absorber constructed from open cell foam. [See Skyner (1992) for more technical details about the flume.]

The motion of the wave paddle is calculated by linear wave theory, according to which we can specify an arbitrary linear sea surface elevation with one spatial dimension, $\eta(x, t)$, as the sum of N Airy waves each with an amplitude a_n, wavenumber k_n, angular frequency ω_n, and initial phase ϵ_n, by the equation

TABLE 1. Initialization parameters for the set of waves examined in the wave flume.

Wave	Wave type	Amplitude, A (m)	Spatial focal point, x_f (m)	Temporal focal point, t_f (s)
1	Plunging	0.143	4.2	15
2	Spilling	0.110	3.6	15
3	Spilling	0.109	3.4	15
4	Nonbreaking	0.107	4.0	15
5	Nonbreaking	0.106	4.0	15
6	Nonbreaking	0.105	4.0	15

$$\eta(x, t) = \sum_{n=1}^{N} a_n \cos(k_n x - \omega_n t + \epsilon_n), \qquad (18)$$

along with the linear dispersion relationship

$$\omega_n^2 = g k_n,$$

where g is the acceleration due to gravity.

Experiments were carried out on the six different waves described in Table 1. The waves used in this study will be referred to by their numbers in the first column of the table. The third column gives the maximum amplitude, $A = \Sigma\, a_n$, of the wave calculated by linear wave theory and the fourth and fifth columns give the focal points (position of maximum amplitude) in space, x_f, and in time, t_f, chosen so that[2] $\epsilon_n = \omega_n t_f - k_n x_f$. These three parameters, together with the shape of the amplitude spectrum, are defining inputs to the program that controlled the wave paddle. The amplitude spectrum for each of the waves in Table 1 is given by

$$a_n = \frac{A}{N}\begin{cases} mf_n + s, & n = 2, \ldots, N-1 \\ (mf_n + s)/2, & n = 1, N, \end{cases}$$

where $m = -0.005\,476$, $s = 0.008\,629$, and

$$f_n = f_1 + (n-1)\delta f,\ n = 1, \ldots, N,$$

where $f_1 = 0.4375$ and $\delta f = 0.03125$.

Knowing the form of the spectrum at a point near the paddle in the flume is not considered directly relevant to this study of the kinematic breaking criterion. Indeed, wave spectra in the frequency domain are global measures over time whereas wave breaking is local in time with effects distributed across frequencies. For the experimental waves, the spectrum produced by, or measured near, the wave paddle will be different from that measured farther down the wave flume. For this reason, detailed descriptions of the spectra of the experimental waves at various positions along the flume are not reported.

Measurements were taken of the surface elevation as a function of distance from the wave paddle and as a function of time from the time of the initial triggering signal to the wave paddle. For this purpose a series of capacitance wave gauges, with electrical resistances giving a linear response to immersion depth (Morrison 1996), were placed at intervals of 0.1 m along the wave flume from 0.4 to 7.5 m from the wave paddle. The surface elevation was recorded from the wave gauges at intervals of 1/16 s for a duration of 32 s from the initial triggering of the wave paddle.

In addition to the surface elevation measurements, fluid particle velocity measurements were made in the wave crests using the PIV technique (Skyner 1992; Quinn 1995). These PIV measurements were made at the positions and times of the start of breaking, (x_v, t_v). PIV is a reliable measurement technique that can yield accurate measurements of the velocity field under breaking and nonbreaking waves. Skyner (1996) has made direct comparisons between PIV measurements of fluid particle velocities and predictions of a numerical model based on the boundary integral method. He found the predicted and measured kinematics to be in good agreement.

The PIV measurement system used in this study is now described. A 15-W argon-ion continuous-wave laser produced a beam directed onto a rotating octagonal mirror and then onto a parabolic mirror. The rate of rotation of the octagonal mirror was adjusted by a rotation speed controller unit to give a time between scans of 1.70 ms. From the parabolic mirror the laser beam was reflected upward through the bottom of the wave flume to give a pulsating light sheet. The water was seeded with neutrally buoyant pollen grains that were illuminated by the pulsating light sheet. PIV images were taken by a Kodak ES1 CCD camera fitted with a Nikon 55-mm lens. The resolution of the CCD camera was 1008×1018 pixels but that of the frame grabber card, which was an Oculus-F/64, was 1024×1024 pixels so all final images had the latter resolution but with narrow blank strips along the left and bottom edges. Opening of the camera shutter was triggered by a signal from the wave paddle controller and the exposure time was sufficiently long to include 3–5 pulses of the light sheet. This yielded individual PIV images of 3–5 exposures of each pollen particle in the field of view as it moved across the image with the flow of the fluid. When analyzed this is equivalent to time averaging each PIV velocity measurement over 5.1–8.5 ms.

Figure 2 shows a PIV image of Wave 3. It is typical of the PIV images of the spilling breakers. The parasitic capillaries beginning to form on the front face, the sharp crest shape, and the streak lines of the seeding particles are all clearly visible.

Each separate PIV image was then analyzed to calculate the fluid particle velocities in the field of view. The analysis was carried out with the aid of a PIV analysis program called EdPIV (Dewhirst 1998, appendix C). EdPIV performs local autocorrelations over a series of cells into which the image is divided. The interro-

[2] These amplitudes predicted by linear theory are significantly different from those measured in the experiments. This is to be expected for highly nonlinear waves.

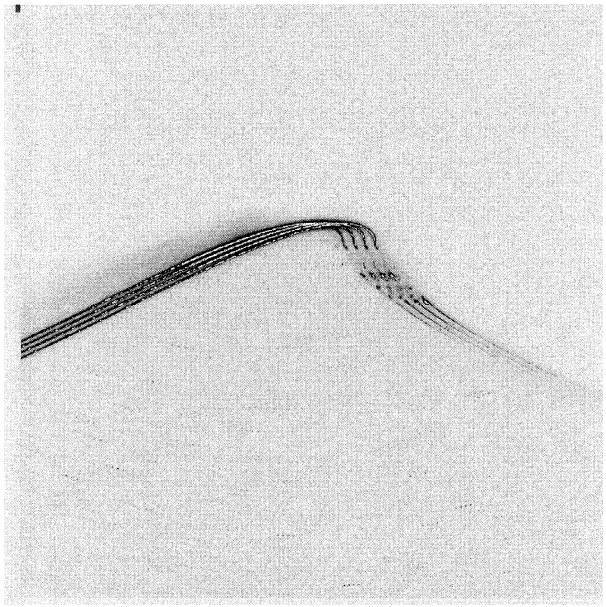

FIG. 2. PIV image of Wave 3 at t_v = 242/16 s. The image shows the parasitic capillaries beginning to form on the front face, the sharper crest shape, and the streak lines of the seeding particles.

gation algorithm employed by EdPIV uses a fixed search window with autocorrelation by FFT and Gaussian peak detection. A velocity vector is obtained for each cell. The choice for the size of the interrogation regions, or cells, is motivated by two factors: that they are large enough to contain the multiple exposures of individual seeding particles as they track across the image and that they a small enough for the velocity vector produced to represent a local measurement. All images in these experiments had dimensions of 1024 × 1024 pixels and were analyzed with interrogation regions of 64 × 64 pixels that overlapped by 32 pixels in both x and z directions, where x is the horizontal distance from the wave paddle and z is the vertical height above mean water level. This gave a 31 × 31 array of velocity vectors for each of the PIV images. Many of these velocity vectors, however, were discarded because they occurred above the fluid surface or because the associated interrogation region crossed the fluid surface or they gave spurious results for some other known reason. Removal of spurious vectors from each image was done by hand, based on the principle of continuity of fluid flow.

b. Errors in the velocity measurements

There are two sources of error that may be of concern in our PIV measurements of fluid velocity in the breaking wave crests. The first is rms error associated with the accuracy of estimation of the location of the displacement correlation peak. The second is downward biasing of the velocity measurement due to gradients in the velocity field. Appropriate references are Keane and Adrian (1990), Huang et al. (1997), Westerweel et al. (1997), and Westerweel (1997).

Generally one would not expect the total velocity measurement error to exceed 2%–3% in well-prepared PIV experiments.

Specifically, we estimate the rms error from Fig. 1 of Westerweel et al. (1997). Typical pixel (px) displacements in our PIV images are about 20 px. Seeding particle image diameters are about 3 px. From Fig. 1 of Westerweel et al. (1997) we see that the expected value of the rms displacement error will be no more than about 0.2 px. This gives an upper bound on the rms error in the velocity measurements of about 1%.

Considering now the velocity biasing from velocity gradients. According to Keane and Adrian (1990, section 5) the dimensionless parameter that represents the performance of PIV with regard to velocity biasing is $M|\Delta\mathbf{u}|\Delta t/d_I$, where M is the magnification in units of px m^{-1}, $|\Delta\mathbf{u}|$ is the maximum variation of the velocity $\mathbf{u}$ in m s^{-1} across the interrogation region of size d_I px, and Δt is the time in seconds between light pulses. The condition given by Keane and Adrian (1990, section 5) for optimum performance of PIV with regard to velocity biasing is

$$\frac{M|\Delta\mathbf{u}|\Delta t}{d_I} < 0.05.$$

Transposing to make $|\Delta\mathbf{u}|$ the subject of the equation we obtain an upper bound on $|\Delta\mathbf{u}|$ given by

$$|\Delta\mathbf{u}| < \frac{0.05 d_I}{M\Delta t}.$$

Calculating the value of the right-hand side for our experiments we have, for Waves 2–6, d_I = 64 px, M = 6489 px m^{-1}, and Δt = 0.001 70 s. This sets the upper bound of $|\Delta\mathbf{u}| < 0.290$ m s^{-1}. The maximum recorded $|\Delta\mathbf{u}|$ from any of the Waves 2–6 is about 0.15 m s^{-1}, well within the optimum limit.

Similarly for Wave 1 we have d_I = 64 px, M = 2473 px m^{-1}, and Δt = 0.006 98 s leading to an upper bound of $|\Delta\mathbf{u}| < 0.185$ m s^{-1}. The maximum recorded $|\Delta\mathbf{u}|$ from Wave 1 is about 0.175 m s^{-1}, which is within the optimum limit.

c. Velocity extrapolation to the free surface

The EdPIV PIV analysis program, as explained in section 4a, yields fluid particle velocities that are averages over interrogation cells that lie wholly within fluid regions. Thus, the velocities are measured close to, but not at, the fluid surface. To obtain the latter, the measured velocities, $u_{\mathrm{PIV}}(z, x, t)$, were extrapolated to the surfaces, $z = \eta_{\mathrm{PIV}}(x, t)$, which were also measured from the PIV images, using the following fitting function

$$u_{\mathrm{fitted}}(z, x, t) = \alpha_1(x, t)\cosh(\alpha_2(x, t) + \alpha_3(x, t)z). \quad (19)$$

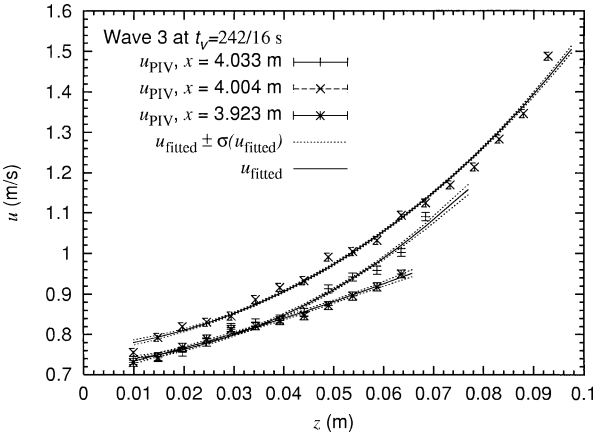

FIG. 3. Graphs of the PIV measured x velocities, u_{PIV}, with their standard deviations, along with the fitted x velocities, u_{fitted}, extrapolated to the positions of the fluid surface, η_{PIV}, for three values of x along Wave 3 at t_v = 242/16 s. Note that the error bars are aligned horizontally in the key but vertically on the plot.

The fitting parameters, α_1, α_2, and α_3, were calculated using the Levenberg–Marquardt method as discussed by Press et al. (1992). The form of the function in Eq. (19) is the same as that obtained from linear wave theory.[3]

The values of $u_{PIV}(z, x, t)$, with $z < \eta_{PIV}(x, t)$, used by the fitting routines were the averages over three PIV images, each taken of exactly the same region of the wave at precisely the same time in its evolution but from three different realizations of the wave. Representative standard deviations, $\sigma(u_{PIV})$, one for each x coordinate, were obtained using all values of u_{PIV} (taken over the range of z coordinate and three PIV images) having the same x and t coordinates. The surface elevations, $\eta_{PIV}(x, t)$, were averages over the three PIV images of each wave. The fitting was performed on each set of averaged u_{PIV} with constant x and t but differing z coordinate. The resulting fitting parameters and their covariances were used in conjunction with Eq. (19) to obtain values for the extrapolated horizontal fluid particle velocities, $u_{fitted}(z = \eta_{PIV}(x, t), x, t)$, along with their standard deviations, $\sigma(u_{fitted})$. Figure 3 shows examples of results obtained by using this fitting procedure on Wave 3 and is representative of the other waves also. It can be seen that the velocities are extrapolated by, at most, about 1 cm into the crest.

Since the fluid velocities crucial to our analysis were measured directly, and did not depend on predictions of a wave theory, any distinction between the use of Stokes' first or second definition of wave speed (see, e.g., Fenton 1985) and the associated frame of reference is unnecessary. The phase speeds were measured in the same reference frame as the fluid velocities. The frame of reference in which the experiments are performed, be it one in which the average Eulerian velocity of the fluid underneath the wave is zero (corresponding to Stokes first definition of wave speed), one in which the total volume flow rate underneath the wave is zero (corresponding to Stokes second definition of wave speed), or any other, is irrelevant to the kinematic breaking criterion. Any relative motion due to a transformation between inertial reference frames would simply add a constant value to both the measured phase speed and the measured fluid particle speed. If the kinematic criterion held in one inertial reference frame, then it would hold in all inertial reference frames.

A simple method, called Wheeler stretching (Wheeler 1970), was used to obtain approximate predictions of fluid particle velocities on the surface of the waves from the wave gauge data. We stress that only the PIV measured velocities are used in the subsequent analyses; the Wheeler approximated values of fluid velocities at the surface, denoted by $u_w(\eta, x, t)$, are only used in some subsequent figures to aid the reader in visualizing the form of the wave outside the small region in which PIV yielded accurate measurements of the velocity.

For Wave 1, standard deviations on the extrapolated horizontal surface fluid particle velocities and the velocities themselves are plotted, along with the surface elevations, in Fig. 4. The standard deviations in the measurements of the surface elevations are extremely small and are not plotted in the figure.

Some of the extrapolated velocity measurements could be checked by hand, directly from the PIV images, by measurements of seeding particles moving very close to the fluid surface. They agreed to within 2% of the extrapolated predictions. For example, measurements made by hand from the PIV photos for Wave 1 at x = 4.141 m and t = 234/16 s and averaged over five laser pulses show that the maximum horizontal fluid particle velocity at the position of maximum curvature of the tip of the crest is as large as 1.38 m s^{-1}, which is almost exactly the result given by the extrapolation. Thus, the authors are satisfied that the method used for extrapolation of the fluid velocities gives accurate values at the water surface.

It is important that the surface elevation data measured by the wave gauges is consistent with that obtained from the PIV measurements and Fig. 4 shows the high level of consistency for Wave 1, given that the wave gauges were placed 0.1 m apart.

d. Calculation of phase velocities for nonlinear waves

Values for each of the three definitions of phase speed given in section 2 were calculated for each wave from the discrete space and time surface elevation samples measured by the wave gauges. A value for the first definition, given by Eq. (2), was calculated from the

[3] From linear theory the x component of the fluid particle velocity under a wave with surface elevation given by $\eta(x, t) = a\cos(kx - \omega t)$ is

$$u(z, x, t) = a\omega \frac{\cosh k(h + z)}{\sinh kh} \cos(kx - \omega t).$$

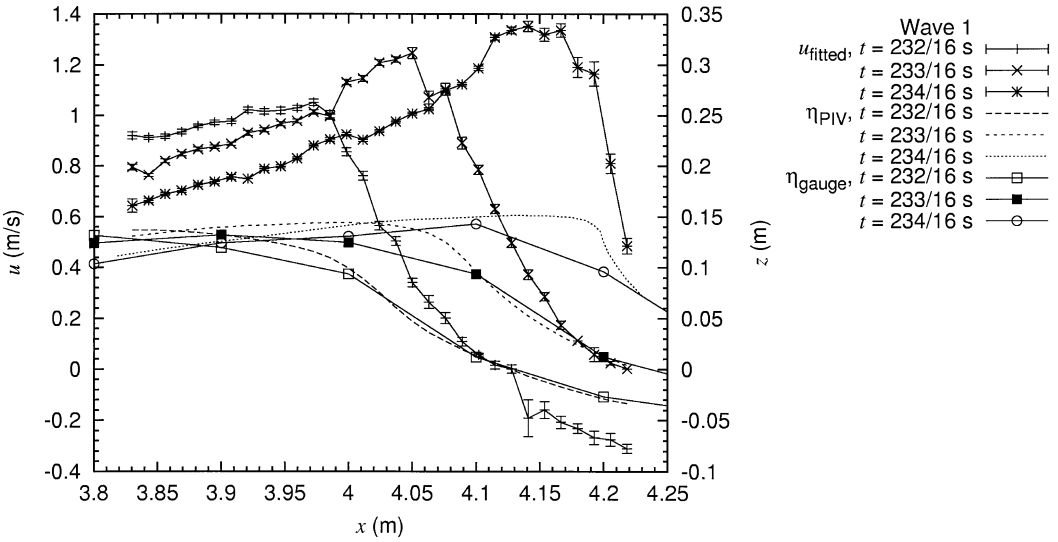

FIG. 4. Extrapolated horizontal surface fluid particle velocities, $u_{\text{fitted}}(z = \eta_{\text{PIV}}, x, t)$, obtained from the PIV images for the plunging breaker labeled Wave 1. Also shown are comparisons of the surface elevations, $\eta_{\text{PIV}}(x, t)$, obtained from the PIV measurements and those obtained from the wave gauge measurements, $\eta_{\text{gauge}}(x, t)$. Note that the error bars are aligned horizontally in the key but vertically on the plot.

zero-downcrossing of the wave profile. The results are given in Table 2.

Values for the third definition of local phase speed, defined by Eq. (15), were found by plotting the positions of the surface elevation maximum, $x_c(t)$, against time over the time interval of 14–15.5 s. In this range the data were fitted to the equation $x_c(t) = a + bt + ct^2$ and the phase speed calculated as $c_p(t) = b + 2ct$. The results of these calculations for $c_p(t)$ for all waves of Table 1 are shown in Table 3.

Values for the second definition, $c_p(x, t)$, given by Eq. (14), were calculated from the discrete partial Hilbert transforms of the surface elevation and their spatial and temporal derivatives. In all the figures showing $c_p(x, t)$ the raw unfiltered calculation results are shown along with results calculated after first low-pass filtering $\eta(x, t)$. The frequency cutoffs for the low-pass filtering were chosen by examination of the corresponding amplitude spectra plotted on a log scale. On a log scale each spectrum showed a high frequency tail that had a constant amplitude, implying that the tail in this region consisted mainly of noise. The values chosen as the frequency cutoffs for low-pass filtering were 6.250 Hz and 4.123 m^{-1}.

TABLE 2. Wavelengths (to nearest 0.1 m), periods (to nearest 1/16 s), and phase speeds of equivalent linear wave for the waves in Table 1.

Wave	Position (m)	Time (s)	Wave-length (m)	Period (s)	Phase speed, c_p (m s^{-1})
1	4.1	234/16	3.6	1.6250	2.22
2	4.0	240/16	3.5	1.5625	2.24
3	4.0	242/16	3.3	1.5625	2.11
4	4.0	237/16	3.3	1.5625	2.11
5	4.0	237/16	3.3	1.5625	2.11
6	4.0	237/16	3.3	1.5625	2.11

1) PLUNGING BREAKER: WAVE 1

For Wave 1 three sets of PIV velocity data were obtained for each of the three times t = 234/16, 233/16, and 232/16 s. We take t_v = 234/16 s, as, with our experimental apparatus, this was the closest we could get ($<$1/32 s) to the time of the start of breaking at t_v. The results of the phase speed calculations for Wave 1 are shown in Figs. 5a–c.

For plunging breaker of Wave 1 the Hilbert transform cannot be calculated if the surface elevations are not single valued, which presents a problem. For this reason the analysis was applied to the wave just before ($<$1/32 s) the front face became vertical. But, of course, shortly after this time the surface elevation becomes triple valued as the wave overturns and this will affect the wave gauge readings. The capacitance gauge data readings will give the height of the surface as the sum of the fluid volume in a column. Thus, as the triple valued surface of the plunging breaker passes around a gauge, the gauge will measure the surface elevation as the sum of the two fluid regions of the wave and not include the air region in contact with the gauge. The triple valued surface function of the wave is effectively collapsed to a single valued function. Another point where some ambiguity in wave gauge measurements may occur is in the whitecap region that occurs after breaking.

Note that, contrary to the case for the extrapolated fluid particle velocities at the surface, simple hand calculations of $c_p(x, t)$ cannot be made from the PIV images. Nevertheless, a value for the nonlocal phase speed

TABLE 3. Fitting parameters and phase speeds defined by Eq. (15) for the waves in Table 1.

Wave	Position (m)	Time (s)	Fitting parameters			Phase speed, $c_p(t)$ (m s^{-1})
			a	b	c	
1	3.8	232/16	−53.926	5.9203	−0.13392	2.03
1	3.9	233/16	−53.926	5.9203	−0.13392	2.02
1	4.1	234/16	−53.926	5.9203	−0.13392	2.00
2	4.0	240/16	−80.073	9.5968	−0.26604	1.61
3	4.0	242/16	−65.459	7.6127	−0.19968	1.57
4	4.0	237/16	−75.858	9.0797	−0.24914	1.70
5	4.0	237/16	−77.821	9.3357	−0.25884	1.69
6	4.0	237/16	−77.596	9.3350	−0.25851	1.68

of the crest can be obtained from the PIV images for Wave 1 from the motion of the (near) vertical front surface. This is not the same as any of the three definitions of phase speed introduced in section 2, but acts as an approximate cross check to the values for phase speed calculated from the wave gauge data according to the definitions of section 2.

2) SPILLING BREAKERS: WAVES 2 AND 3

The situation for the spilling breakers, Waves 2 and 3 of Table 1, was slightly different from that of the plunging breaker of Wave 1 in that the surface elevations were never double valued, and therefore we expect the surface elevation data from the wave gauges to be more accurate leading to more precise calculations of the partial Hilbert transforms and hence local phase speed, $c_p(x, t)$. The only point where some ambiguity in wave gauge measurements may have occurred is in the whitecap region, but this is expected to be slight for the limited whitecap produced in the wake of the spilling breakers.

The results of the phase speed calculations for Waves 2 and 3 at their start times for breaking, $t_v = 240/16$ and 242/16 s, respectively, are shown in Figs. 5d and 5e.

3) NONBREAKING WAVES: WAVES 4, 5, AND 6

For the nonbreaking Waves 4, 5, and 6 of Table 1 the surface elevations were never double valued, neither were there any whitecaps so we expect the surface elevation data from the wave gauges to be the most accurate of the three wave types leading to the most precise calculations of the partial Hilbert transforms and hence local phase speed, $c_p(x, t)$.

The results of the phase speed calculations for Waves 4, 5, and 6 at their times for maximum amplitudes, $t = 237/16$ s, are shown, respectively, in Figs. 6a–c.

5. Discussion

The relationship between the phase speed and the horizontal fluid velocity at the surface of breaking waves has been investigated. Three different definitions of phase speed were used: the nonlocal definition given by Eq. (2) and defined to be equal to that of the equivalent linear wave, the truly local definition based on the partial Hilbert transforms of the surface elevation and given by Eq. (14), and finally the definition based on the observed speed of the surface elevation maximum at the crest and given by Eq. (15). Statements made in the literature, for example, those highlighted in the introduction, suggest that experiments should confirm the hypothesis that the horizontal fluid velocity at the surface of the breaking waves, Waves 1, 2, and 3 of Table 1, would exceed the phase speed for at least one of the definitions used. The contrary was found to be true for each of the waves in Table 1 and for each of the three definitions of phase speed used in this study. The results are summarized in Table 4. One would expect the ratio $u_{\mathrm{PIV}}/c_p(x, t)$ in the last column to be at least unity if the kinematic breaking criterion was valid for these waves.

The first wave data analyzed were from the plunging breaker Wave 1. The large fluctuations in the unfiltered results for $c_p(x, t)$ are not noise. They occur at positions of negative maxima and positive minima in the surface profile (Melville 1983, section 4.3). It was therefore deemed preferable to retain all the measured frequencies in the analysis even though low-pass filtered results for $c_p(x, t)$ are also shown in the figures. The high frequencies are certainly necessary to correctly represent the sharp crests associated with the breaking waves.[4]

From Table 4 it is evident that, for Wave 1, the local phase speed is significantly greater than the horizontal surface particle velocity at, and shortly before, the point of breaking. This is the case for each of the definitions of phase speed. At the breaking point, (x_v, t_v), the lowest value of local phase speed is seen to be given by the unfiltered local phase speed as defined by Eq. (14). This lowest value is 1.67 m s^{-1}. The local phase speed calculated from the linear approximation is about 33% greater, and that calculated from the rate of change in

[4] It should be noted that examination of the Fourier amplitude spectra of the surface elevations showed that the Fourier contributions at the Nyquist frequencies (8 Hz and 5 m^{-1}) for the sampling rates used were very small, being in both cases about 10^{-4} times the Fourier component of maximum amplitude. Thus, these sampling rates are short enough to resolve most of the frequencies in the wave evolution process and there is very little aliasing in any of the spectra.

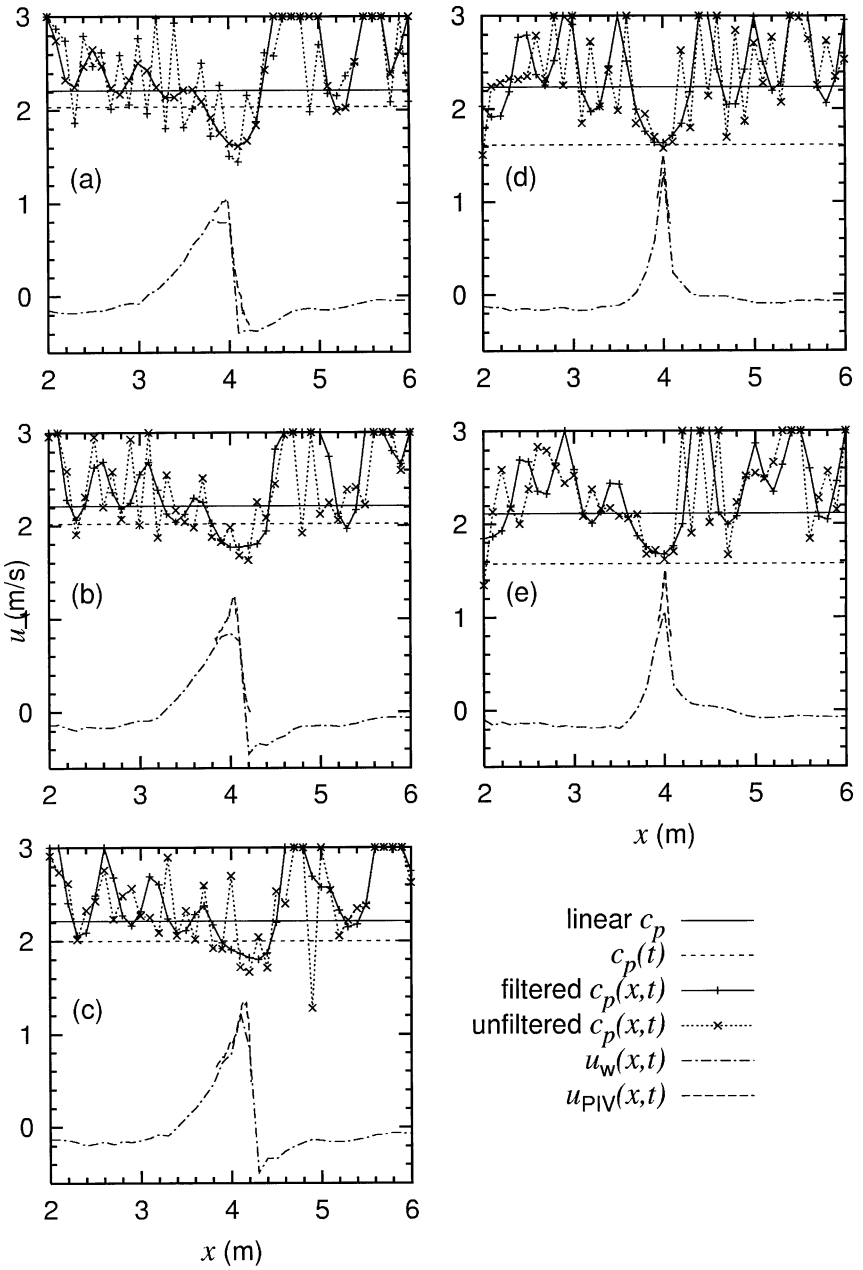

FIG. 5. Comparisons of the three definitions of phase speed with horizontal fluid particle velocities at the surface, $u_{\text{PIV}}(z = \eta_{\text{PIV}}, x, t)$, obtained from PIV measurements. Wave 1 at times (a) t = 232/16 s, (b) t = 233/16 s, and (c) t_v = 234/16 s; Wave 2 at (d) t_v = 240/16 s and Wave 3 at (e) t_v = 242/16 s. Also shown are the Wheeler stretched predictions for the horizontal fluid particle velocities at the surface $u_w(z = \eta_{\text{gauge}}, x, t)$.

position of the maximum of $\eta(x, t)$ is about 20% greater. For Wave 1 the greatest ratio obtained between the horizontal fluid particle velocity in the crest and the local phase speed is about 0.81 at (x_v, t_v). This is significantly less than the proposed breaking criterion value of unity.

As explained in section 4d(1), there will be some error in calculating the partial Hilbert transforms of the surface elevation for a plunging breaker since the surface elevation is not a mathematical function in the strict sense; that is to say, it is not single valued as the wave overturns. The wave gauges, however, can never yield anything other than a single valued function and this is used to calculate the partial Hilbert transforms of the wave gauge data and, hence, $c_p(x, t)$.

The second wave type analyzed were the spilling breakers, Waves 2 and 3. For these waves the problem of the surface elevation becoming triple valued is eliminated, but, since a foam whitecap zone exists just after

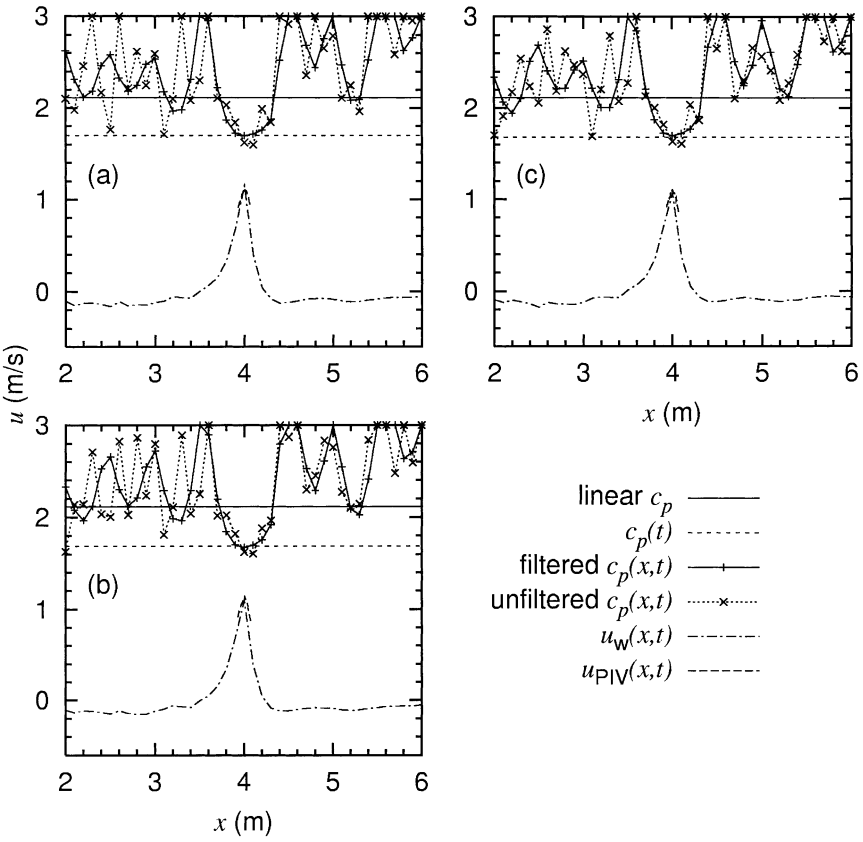

FIG. 6. As in Fig. 5 but (a), (b), and (c) show Waves 4, 5, and 6, each at time $t = 237/16$ s.

breaking, there may be some small error introduced into the partial Hilbert transform calculations and the calculations of their derivatives due to slight ambiguity in the position of the fluid surface within the whitecap.

Figures 5d and 5e show that at the point of breaking for the spilling breakers the local phase speed based on the partial Hilbert transforms (unfiltered) and the definition using the rate of change in position of the maximum of $\eta(x, t)$ both give approximately the same value for the local phase speed. The values obtained from the equivalent linear wave approximations are significantly greater, by about 42% and 30% for Waves 2 and 3, respectively. For both of the spilling breakers the maximum horizontal fluid particle velocity at the tip of the crest is about 6% less than the local phase speeds $c_p(x, t)$ or $c_p(t)$.

For the nonbreaking waves, Waves 3, 4, and 5, a result similar to that for the spilling breakers is obtained in that the two local definitions of phase speed give similar values at the crest, although the unfiltered calculation based on Eq. (14) is consistently lower, by about 5%, than that based on Eq. (15). Also, as with all the previous waves, the value of phase speed calculated from the equivalent linear wave definition gives a poor approx-

TABLE 4. Values of the phase speed calculated from the various definitions given in section 2 compared with the values of the horizontal fluid particle velocities extrapolated from PIV measurements to the surface of the crest.

Wave	Time (s)	Maximum extrapolated u_{PIV} (m s^{-1})	Phase speeds (m s^{-1})			Breaking criterion ratio $u_{PIV}/c_p(x, t)$
			Linear c_p	Crest $c_p(t)$	Min. Hilbert $c_p(x, t)$	
1	232/16	1.05 at 3.973 m	2.22	2.03 at 3.8 m	1.45 at 4.1 m	0.72
1	233/16	1.25 at 4.050 m	2.22	2.02 at 3.9 m	1.63 at 4.2 m	0.77
1	234/16	1.35 at 4.141 m	2.22	2.00 at 4.1 m	1.67 at 4.2 m	0.81
2	240/16	1.50 at 3.999 m	2.24	1.61 at 4.0 m	1.58 at 4.0 m	0.95
3	242/16	1.51 at 4.004 m	2.11	1.57 at 4.0 m	1.62 at 4.0 m	0.93
4	237/16	1.11 at 3.994 m	2.11	1.70 at 4.0 m	1.60 at 4.1 m	0.70
5	237/16	1.13 at 3.999 m	2.11	1.69 at 4.0 m	1.60 at 4.1 m	0.71
6	237/16	1.10 at 3.999 m	2.11	1.68 at 4.0 m	1.61 at 4.1 m	0.68

imation to the value calculated locally at the crest. For the nonbreaking waves the discrepancy between phase speed calculated from the equivalent linear wave definition and that obtained from the two local definitions is about 32%.

Comparing the results for the plunging and spilling breakers, we see that the kinematic breaking criterion is closer to being satisfied in the crest of the spilling breaker. This may be explained by recalling the point, made in section 3b, that the ratio of horizontal fluid particle velocity to local phase speed must be unity at any point on the wave surface where the radius of curvature is zero. The radius of curvatures at the tips of the crests of the spilling breakers are less than those of the plunging breaker at the time, t_v, of incipient breaking.

Applying a basic hydrodynamic principle, namely the kinematic free surface boundary condition, it can be shown that, on the surface of the vertical front face of a breaking wave at the point (x_v, t_v), the x velocity component of the fluid particles, $u[\eta(x_v, t_v), x_v, t_v]$, is exactly equal to x velocity component of that point on the surface given by $\eta(x_v, t_v)$. But this statement is of no use as a breaking criterion. For a kinematic breaking criterion to have any predictive value it would require that the $u(\eta(x, t), x, t)$ was equal to or greater than the fluid surface speed before the occurrence of a vertical front face, that is to say, Eq. (1) would hold for some definition of phase velocity $c_p(x, t)$. We have not found this criterion to be satisfied for any of our definitions c_p, $c_p(x, t)$, or $c_p(t)$ given by Eqs. (2), (4), and (15).

For breaking to occur it is certainly not a logical requirement for Eq. (1) to hold. Consider, by way of analogy, a length of taut elastic material. Let the longitudinal axis be the x direction and the transverse axis of interest be the z direction. Consider a transverse wave propagating in the positive x direction along the length of elastic. It is quite possible for the x component of the velocity of the material of elastic to be identically zero for all time and all positions along the elastic. The transverse wave motion is produced entirely by the z component of the velocity of the elastic material, yet the wave itself has a phase speed in the x direction that is not zero. In a similar way the z-velocity component of the fluid in a water wave can increase or decrease the x component of the water wave's phase velocity. In the water wave the fluid particles preceding the front face of a wave are ascending and as, before breaking, the front face must be at an angle less that 90° to the horizontal, this upward motion of fluid particles contributes to the forward motion of the angled surface of the wave. Thus, increasing the value of the phase velocity in the direction of travel of the surface wave regardless of the fluid particle velocity in the x direction. Only when the front face is vertical does any z component of the fluid particle velocity have no effect on the phase speed of surface wave. In this case $u[\eta(x_v, t_v), x_v, t_v]$ is exactly equal to the phase velocity of the wave at that point (but it does not exceed it).

It is interesting to note that in all waves analyzed in the wave flume the local phase speed has its lowest minimum in the vicinity of the focal point of the wave, which is where one would expect the surface velocities to be greatest. Also, note that the variation of $c_p(x, t)$ shows that the rear surface is traveling faster than the front surface in the figures for Wave 1, implying that this wave is still ''bunching up'' while evolving to a plunging breaker, whereas for the spilling breakers $c_p(x, t)$ is almost symmetrical about the focal point, implying that the wave is at its (spilling) breaking point.

Thus, for all the waves in this study the maximum horizontal fluid particle velocities on the surfaces of the crests are consistently less than the associated phase speeds. The expected errors of 2%–3% in the PIV velocity measurements are not enough to account for the measured discrepancies between $u(\eta, x, t)$ and any of the phase speed definitions if the kinematic breaking criterion were true. An error of about 20% would be required to satisfy the kinematic breaking criterion of the plunging breaker, Wave 1. For the spilling breakers, Waves 2 and 3, satisfying the kinematic breaking criterion was missed by about 6%. Our experimental results, therefore, are found to be consistent with all but one of the studies reviewed previously in section 3. The one exception being Chang and Liu (1998), who use linear theory to obtain $u[\eta(t), t]$ from single point measurements of $\eta(t)$.

6. Conclusions

In this study we have attempted to assess the sufficiency of each of three definitions of wave phase speed with regard the kinematic breaking criterion, which states that the breaking of water waves implies the horizontal velocities of the fluid particles in the breaking crest exceed the phase speed of the breaking crest at, or before, the point of breaking [see Eq. (1)].

For each of the waves studied we found that the phase speeds calculated from the equivalent linear waves give poor approximations to the values obtained by using any of the local phase speed definitions. Moreover, we found that, with each of these three definitions of phase speed, the kinematic breaking criterion is not satisfied and is therefore not universal. For the plunging breaker the criterion is far from satisfied. For the spilling breaker the criterion is closer to being satisfied, but is not, even within the limits of experimental error. It is concluded that the truth of the condition $u(\eta, x, t)/c_p(x, t) > 1$ in a wave crest, at or before the first occurrence of a vertical tangent to the forward face, may be a sufficient condition for breaking but it is not a necessary condition. On the evidence of the results presented here, we suggest that, unless and until a local definition of phase speed is devised for which no instances can be found that

falsify the kinematic breaking criterion, this criterion be abandoned as a universal predictor of wave breaking.

Acknowledgments. We would like to thank Prof. Clive A. Greated for making the Edinburgh wave flume facilities available to us for use in these experiments. We would also like to thank Narumon Emarat and Tom Haydon at Edinburgh University for their advice and assistance in performing the experiments. Thanks are also due to the reviewers of this paper whose contributions have led to significant improvements. This work was supported by the Natural and Environmental Research Council in the form of a ROPA.

REFERENCES

Baldock, T. E., C. Swan, and P. H. Taylor, 1996: A laboratory study of nonlinear surface waves on water. *Philos. Trans. Roy. Soc. London,* **354A,** 649–676.

Banner, M. L., and D. H. Peregrine, 1993: Wave breaking in deep water. *Annu. Rev. Fluid Mech.,* **25,** 373–397.

——, and X. Tian, 1998: On the determination of the onset of breaking for modulating surface gravity water waves. *J. Fluid Mech.,* **367,** 107–137.

Chang, K.-A., and P. L.-F. Liu, 1998: Velocity, acceleration and vorticity under a breaking wave. *Phys. Fluids,* **10,** 327–329.

Cokelet, E. D., 1977: Steep gravity waves in water of arbitrary uniform depth. *Philos. Trans. Roy. Soc. London,* **286A,** 183–230.

Dewhirst, T. P., 1998: Multiple CCD array digital particle image velocimetry. Ph.D. thesis, University of Edinburgh, 220 pp.

Fenton, J. D., 1985: A fifth-order Stokes theory for steady waves. *J. Waterway, Port, Coastal Ocean Eng.,* **111,** 216–234.

Gudmestad, O. T., 1993: Measured and predicted deep water wave kinematics in regular and irregular seas. *Mar. Struct.,* **6,** 1–73.

——, J. M. Johnsen, J. Skjelbreia, and A. Tørum, 1988: Regular water wave kinematics. *Boss '88—Behaviour of Offshore Structures,* Elsevier Science, 789–803.

Huang, H., D. Dabiri, and M. Gharib, 1997: On error of digital particle image velocimetry. *Meas. Sci. Technol.,* **8,** 1427–1440.

Hwang, P. A., D. Xu, and J. Wu, 1989: Breaking of wind-generated waves: Measurements and characteristics. *J. Fluid Mech.,* **202,** 177–200.

Keane, R. D., and R. J. Adrian, 1990: Optimization of particle image velocimeters. Part I: Double pulsed systems. *Meas. Sci. Technol.,* **1,** 1202–1215.

Kinsman, B., 1984: *Wind Waves: Their Generation and Propagation on the Ocean Surface.* Dover, 676 pp.

Kjeldsen, S. P., 1989: The experimental verification of numerical models of plunging breakers. *Proc. 19th Int. Conf. on Coastal Engineering,* Houston, TX, Amer. Soc. Civil Eng., 15–30.

——, 1990: Breaking waves. *Water Wave Kinematics,* A. Tørum and O. T. Gudmestad, Eds., Series E: Applied Sciences, NATO Advanced Scientific Institute Series, Vol. 178, Kluwer Academic, 453–473.

Longuet-Higgins, M. S., 1978a: The instabilities of gravity wave of finite amplitude in deep water. I. Superharmonics. *Philos. Trans. Roy. Soc. London,* **360A,** 471–488.

——, 1978b: The instabilities of gravity wave of finite amplitude in deep water. II. Subharmonics. *Philos. Trans. Roy. Soc. London,* **360A,** 489–505.

——, and E. D. Cokelet, 1976: The deformation of steep surface waves on water. I. A numerical method of computation. *Proc. Roy. Soc. London,* **350A,** 1–26.

——, and ——, 1978: The deformation of steep surface waves on water. II. Growth of normal mode instabilities. *Proc. Roy. Soc. London,* **364A,** 1–28.

——, and R. P. Cleaver, 1994: Crest instabilities of gravity waves. Part 1: The almost-highest wave. *J. Fluid Mech.,* **258,** 115–129.

——, and D. G. Dommermuth, 1997: Crest instabilities of gravity waves. Part 3. Nonlinear development and breaking. *J. Fluid Mech.,* **336,** 33–50.

——, and M. Tanaka, 1997: On the crest instabilities of steep surface waves. *J. Fluid Mech.,* **336,** 51–68.

Melville, W. K., 1983: Wave modulation and breakdown. *J. Fluid Mech.,* **128,** 489–506.

——, and R. J. Rapp, 1988: The surface velocity field in steep and breaking waves. *J. Fluid Mech.,* **189,** 1–22.

Morrison, I. G., 1996: The hydrodynamic performance of an oscillating water column. Ph.D. thesis, University of Edinburgh, 164 pp.

New, A. L., P. McIver, and D. H. Peregrine, 1985: Computations of overturning waves. *J. Fluid Mech.,* **150,** 233–251.

Perlin, M., J. He, and L. P. Bernal, 1996: An experimental study of deep water plunging breakers. *Phys. Fluids,* **8,** 2365–2374.

Poularikas, A. D., Ed.,1995: *The Transforms and Applications Handbook.* CRC Press, 1120 pp.

Press, W. H., S. A. Teukolsky, W. T. Vetterling, and B. P. Flannery, 1992: *Numerical Recipes in FORTRAN.* Cambridge University Press, 963 pp.

Quinn, P. A., 1995: Breaking waves on beaches. Ph.D. thesis, University of Edinburgh, 166 pp.

Rankine, W. J. M., 1864: Summary of the properties of certain streamlines. *Philos. Mag.,* **XXVII,** 282–288.

Skjelbreia, J. E., G. Berek, Z. K. Bolen, O. T. Gudmestad, J. C. Heideman, R. D. Ohmart, and N. Spidsoe, 1991: Wave kinematics in irregular waves. *Proceedings of Offshore Mechanics and Arctic Engineering,* Vol. 1A, ASME, 223–228.

Skyner, D. J., 1992: The mechanics of extreme water waves. Ph.D. thesis, University of Edinburgh, 242 pp.

——, 1996: A comparison of numerical predictions and experimental measurements of the internal kinematics of a deep-water plunging wave. *J. Fluid Mech.,* **315,** 51–64.

Tulin, M. P., and J. J. Li, 1992: On the breaking of energetic waves. *Int. J. Offshore Polar Eng.,* **2,** 46–53.

Vinje, T., and P. Brevig, 1981: Numerical simulation of breaking waves. *Adv. Water Resour.,* **4,** 77–82.

Westerweel, J., 1997: Fundamentals of digital particle image velocimetry. *Meas. Sci. Technol.,* **8,** 1379–1392.

——, D. Dababiri, and M. Gharib, 1997: Effect of a discrete window offset on the accuracy of cross-correlation analysis of digital PIV recordings. *Exp. Fluids,* **23,** 20–28.

Wheeler, J. D., 1970: Method for calculating forces produced by irregular waves. *J. Pet. Technol.,* **22,** 359–367.